Separation and Purification Technology 332 (2024) 125752

Contents lists available at ScienceDirect

Separation and Purification Technology

journal homepage: www.elsevier.com/locate/seppur

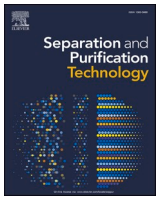

Polysulfone ultrafiltration membranes fabricated from green solvents: Significance of coagulation bath composition

Cannon Hackett [a], David Hale [a], Brianna Bair [a], God's-Delight Manson-Endeboh [c], Xiaolei Hao [b], Xianghong Qian [b], S. Ranil Wickramasinghe [a], Audie Thompson [d,*]

[a] Ralph E. Martin Department of Chemical Engineering, University of Arkansas, Fayetteville, United States
[b] Department of Biomedical Engineering, University of Arkansas, Fayetteville, United States
[c] Department of Science and Math, NorthWest Arkansas Community College, Bentonville, United States
[d] U.S. Army Engineer Research and Development Center, Vicksburg, United States

ARTICLE INFO

Editor: T. Kuo-Lun

Keywords:
Sustainable
Morphology
Green solvent
Phase inversion

ABSTRACT

Even though membranes can lead to more environmentally sustainable separation processes, membrane casting typically involves toxic organic solvents. Recently, there has been increasing interest in substituting these toxic solvents for green solvents. In this study, polysulfone ultrafiltration membranes were fabricated by nonsolvent induced phase separation using two green, bio-derived solvents: Cyrene and gamma-valerolactone (GVL). The effect of coagulation bath composition was investigated, with water, ethanol, and water/ethanol mixtures tested as nonsolvents in the bath. Membranes were characterized and their performance was tested by dead-end filtration. For both Cyrene and GVL, using pure water in the coagulation bath resulted in membranes with residual solvent trapped inside. During dead-end filtration, these membranes were either impermeable (in the case of GVL) or had very low bovine serum albumin (BSA) rejection (in the case of Cyrene). Concentrations of ~ 50–75 v% ethanol in the coagulation bath led to improved solvent removal and better pore formation, as indicated by scanning electron microscopy. These membranes also had higher flux and rejection. For example, membranes cast using Cyrene with a 65:35 volumetric ratio of ethanol:water in the coagulation bath achieved 70.1 L/m^2/h water flux at 2.41 bar and 96.7 % BSA rejection. Additionally, the effect of humidity on membranes cast using GVL was investigated. Membranes cast under moderate humidity had novel surface morphologies with porous dimples ~ 1 μm wide. Overall, these results show that Cyrene and GVL are promising solvents for preparing polysulfone ultrafiltration membranes. The work highlights the importance of relating membrane properties to casting conditions.

1. Introduction

Ultrafiltration (UF) is a mature technology routinely used for the removal of dissolved and suspended solutes in the size range 2–100 nm. Species that are rejected by the membrane include viruses, bacteria, proteins, and colloidal particles [1–3]. UF plays a vital role in many industries, including food and beverage production, water purification, and pharmaceutical manufacturing [3]. While ceramic UF membranes are available, polymers are commonly used. Polymeric membranes are often fabricated by nonsolvent induced phase separation (NIPS) [4]. In this process, a polymer is dissolved in a solvent, then formed into the desired shape (e.g., a sheet or hollow fiber), which is then immersed in a coagulation bath containing nonsolvent. The exchange of solvent in the dope solution with nonsolvent in the bath induces phase inversion, leading to the formation of a porous membrane.

Membrane processes are frequently claimed to be green, sustainable unit operations. Although membrane processes benefit from potentially high efficiencies and low energy consumption, there are toxicological and environmental concerns associated with the solvents used in membrane fabrication. In fact, membrane manufacturing methods frequently make use of hazardous organic solvents that are not "green". For typical polymers such as polysulfone (PSf), polyethersulfone (PES), and polyacrylonitrile (PAN), the solvents most commonly used in the NIPS process are N-methylpyrrolidone (NMP), N,N-dimethylacetamide (DMAc), and N,N-dimethylformamide (DMF) [4]. Of these, NMP is a reproductive and developmental toxin [5,6], while DMAc and DMF have

* Corresponding author.
E-mail address: audie.k.thompson@usace.army.mil (A. Thompson).

https://doi.org/10.1016/j.seppur.2023.125752
Received 17 August 2023; Received in revised form 14 November 2023; Accepted 15 November 2023
Available online 20 November 2023

been found to cause liver damage and developmental harm [7–9]. These solvents are becoming increasingly heavily regulated due to their toxicity. In the European Union, NMP, DMAc, and DMF are classified as substances of very high concern under the Registration, Evaluation, Authorisation & Restriction of Chemicals (REACH) regulation, which limits industrial usage [10]. Meanwhile, in the United States, the Environmental Protection Agency found, in a 2022 revision to a risk determination, that NMP "presents an unreasonable risk of injury to health when evaluated under its conditions of use", paving the way for further regulations [11]. Additionally, environmental concerns arise since membrane manufacturing is estimated to produce 50 billion liters of solvent-contaminated wastewater annually [12]. Up to 69 % of the wastewater is not treated before disposal, but is sent down the drain as-is or with dilution, according to a survey of membrane manufacturers [12].

These safety, regulatory, and environmental challenges have prompted researchers to investigate alternative green solvents for use in membrane fabrication. Green solvents have less toxicity and environmental impact compared to traditional solvents. Numerous green solvents have been investigated, including Cyrene, gamma-valerolactone (GVL), Polarclean, methyl lactate, ionic liquids, deep eutectic solvents, and organic carbonates [13]. Here, we focus specifically on Cyrene and GVL. Given the significant effect solvent properties have on membrane morphology, switching to a new solvent is not trivial.

Cyrene (dihydrolevoglucosenone) is a recently developed solvent, first described in 2014, which is produced from cellulose [14]. The solubility properties of Cyrene are similar to NMP, although Cyrene's viscosity is notably higher, at 14.5 cP [15], compared to 1.7 cP for NMP [16]. Cyrene does not possess known carcinogen, mutagen, or reprotoxic characteristics, and has a very low acute toxicity (LD_{50}) of $>$ 2000 mg kg^{-1} [15]. Research groups have used Cyrene to fabricate membranes from a variety of polymers including polysulfone (PSf) [17–19], polyethersulfone (PES) [19–23], poly(vinylidene fluoride) (PVDF) [19,20], polyimide [19], cellulose acetate [19,24], cellulose triacetate [24], and polyhydroxyalkanoate [25].

Several studies have investigated Cyrene as a solvent for fabricating PSf membranes. PSf is one of the most common polymers utilized to make membranes and has the advantages of good mechanical, thermal, and chemical stability [4]. Bridge et al. [17] fabricated PSf gas separation membranes by a combined dry/wet casting methodology. Cyrene was used as a co-solvent in the dope solution, along with tetrahydrofuran and ethanol. During phase inversion, the use of Cyrene led to delayed demixing, which suppressed macrovoid formation. Milescu et al. [19] casted PSf membranes by NIPS from a solution of 15 wt% PSf in Cyrene. They tested membrane performance by dead-end filtration with water, finding that the membranes achieved a water flux of up to 172.9 L/m^2/h (LMH) at 5 bar. However, no filtration tests were performed using a model solute, so the membranes' ability to reject solutes is unknown. This is particularly important given the strong influence membrane morphology has on its performance. Foong et al. [18] casted PSf membranes by NIPS, from a dope solution of 18 wt% PSf in Cyrene. The membranes had an undesirable wrinkled texture, so for the rest of the study, Cyrene was abandoned in favor of other solvents. In all three of these studies, water was employed as the nonsolvent in the coagulation bath. The difficulties encountered by Foong et al. raise the question of whether using a different coagulation bath composition might improve membrane morphology and performance [18].

GVL is another green solvent, which has some similarities to Cyrene. Like Cyrene, GVL is derived from biomass, and has very low toxicity [26,27]. In fact, GVL is used in perfumes and as a food additive [26]. GVL also has a solubility profile similar to NMP, and a comparable viscosity of 2.2 cP [15]. GVL has been used to fabricate membranes from PSf [28–31], PES [30,31], polyimide [30,31], cellulose acetate [30,31], and cellulose triacetate [30,31]. Dong et al. [28,29] attempted to make PSf membranes using GVL as the solvent and water as the nonsolvent in the coagulation bath. However, they encountered problems when using these fabrication parameters. The resulting membranes were nearly impermeable, with a water flux less than 0.6 LMH at 4 bar. Additionally, the membranes "would stick to themselves like glue". These problems were resolved by using cosolvent blends of GVL and Polarclean, instead of only GVL. Membranes made using the cosolvent blends had drastically improved fluxes of up to 750 LMH at 4 bar. Rasool and Vankelecom [30,31] fabricated PSf nanofiltration membranes using GVL as the solvent, with dope solutions of 10–20 wt% PSf in GVL. Coagulation baths of either pure water or pure ethanol were used. After fabrication, membranes were tested by filtration with a rose Bengal solution. Membranes cast from 10 wt% PSf were defective, with very low (~5%) rose Bengal rejection. Meanwhile, membranes cast from 15 to 20 % PSf in GVL had relatively low fluxes of 20 LMH/bar or less. The mixed results from these studies – especially the comment from Dong et al. about membranes sticking together like glue when GVL was used as the solvent – suggest that the PSf/GVL dope solution may have poor compatibility with water in the coagulation bath [28,29]. This again raises the possibility of improving membrane morphology and performance by using a different bath composition.

Membrane morphology is strongly affected by the composition of the coagulation bath. Additives such as acids, bases, and salts can be added to a water coagulation bath to influence various membrane properties including permeability, solute rejection, and hydrophilicity [32–37]. For instance, coagulation baths of water with dissolved KCl salt were found to improve flux and hydrophilicity for polyvinyl chloride/bentonite UF membranes [33]. Additionally, the bulk nonsolvent can be changed. Although water is the most commonly used nonsolvent in this role, the effect of using other nonsolvents has been investigated in numerous studies [38–40]. For example, Zuo et al. [38] casted PVDF membranes, using DMAc as the solvent and varying the nonsolvent in the coagulation bath. Membranes cast into water had a finger-like morphology, while those cast into alcohols (methanol, ethanol, and isopropanol) developed a sponge-like morphology due to delayed demixing. Also, several studies have used ethanol/water mixtures in the coagulation bath [41–43]. Effects of ethanol concentration on the resulting membranes varied depending on the exact system. For some dope solutions, such as PVDF/DMF and functionalized-PSf/DMF, increasing concentrations of ethanol in the bath led to membranes with larger pores and higher flux [41,42]. Meanwhile, for a dope solution of PVDF/DMAc, increasing concentrations of ethanol in the coagulation bath produced membranes with lower porosity and reduced flux [43].

In summary, substantial investigation has been done in two areas: first, the use of green solvents (such as Cyrene and GVL) for membrane fabrication, and second, the effects of coagulation bath composition on membrane properties. However, little has been done at the intersection of these two research areas. Since several of the studies referenced above have noted problems with using Cyrene or GVL to fabricate membranes, it is worthwhile to investigate whether these problems can be resolved by making a simple change to the fabrication protocol. In this study, we tested whether using a mixed ethanol/water coagulation bath instead of a pure water coagulation bath is a viable solution that would lead to membranes with improved filtration performance.

In addition, there are gaps in the research on the ultrafiltration performance of membranes fabricated from Cyrene and GVL. At the time of writing, for membranes cast from Cyrene or GVL (not part of a cosolvent mixture), we were unable to find any studies which provided rejection data for model solutes such as BSA, polyethylene glycol (PEG), or dextran. These solutes are routinely used to characterize UF membranes. Here, we aimed to explore the ultrafiltration performance of membranes fabricated from Cyrene and GVL to evaluate whether these solvents can adequately replace traditional solvents.

In this study, PSf ultrafiltration membranes were fabricated by NIPS, using either Cyrene or GVL as the solvent. We choose to study PSf as it is one of the most commonly used polymers. PSf membranes are used in many industries ranging from biomedical applications, bioseparations,

food and beverage production, and water treatment. During membrane fabrication, the composition of the coagulation bath was varied: pure water, pure ethanol, and mixtures of water and ethanol at various concentrations were tested. Membranes were characterized to determine pore morphology and the degree of solvent removal from the membrane. Performance was evaluated using dead-end filtration. Additionally, cloud point experiments were performed to help elucidate mechanisms behind differences in morphology and performance between membranes. Membrane morphology was compared to membrane performance.

2. Experimental

2.1. Materials

Cyrene, gamma-valerolactone (GVL), sodium phosphate dibasic (anhydrous), sodium phosphate monobasic (monohydrate), and sodium hydroxide were purchased from Sigma-Aldrich (St. Louis, MO). Potassium dihydrogen phosphate was purchased from Beantown Chemical (Hudson, NH). Polysulfone (60,000 M.W.) was purchased from Acros Organics (Geel, Belgium). Ethanol (pure, 200 proof) was purchased from Decon Labs (King of Prussia, PA). Methanol was purchased from MilliporeSigma (Burlington, MA). Sulfhydryl-blocked bovine serum albumin (BSA) was purchased from Lee Biosolutions (Maryland Heights, MO). 1 kDa, 10 kDa, 40 kDa, 70 kDa, and 500 kDa dextrans were purchased from Pharamacosmos (Holbaek, Denmark). 4 kDa dextran was purchased from Serva (Heidelberg, Germany). Ultracel regenerated cellulose UF membranes with a 30 kDa molecular weight cutoff (MWCO) were provided by MilliporeSigma (Burlington, MA). All water used was deionized (DI).

2.2. Membrane fabrication and treatment

PSf membranes were fabricated by NIPS. First, dope solutions of 12 wt% PSf in Cyrene and 15 wt% PSf in GVL solutions were prepared in a sealed Erlenmeyer flask. The polymer concentration was higher in GVL solutions than in Cyrene solutions to compensate for the fact that GVL is less dense than Cyrene (1.05 vs. 1.25 g/mol) and has a much lower viscosity than Cyrene (2.2 cP vs. 14.5 cP) [15]. The solutions were mixed on a hot-plate at 100 °C (for Cyrene solutions) or 66 °C (for GVL solutions) until the PSf was dissolved (6–8 h). Then, the solutions were degassed by allowing the flasks to sit overnight at room temperature (21 ± 3 °C). Next, a film of polymer dope solution was cast on a glass plate using a doctor blade set to 250 μm. (The film shrinks during NIPS. Final thicknesses are provided in section S1 of the supplementary information.) After 10 s, the plate was submerged in a coagulation bath of either water, ethanol, or a water/ethanol mixture. Membranes were left in the coagulation bath for 4 h after casting, then stored in water until further testing. Batches of membranes were named based on the solvent used and the volumetric ratio of ethanol in the coagulation bath (Table 1). For example, the Cyr25 membranes were cast from a 12 wt% PSf in Cyrene solution, into a coagulation bath composed of a 25:75 volumetric ratio of ethanol to water. We originally chose volumetric ratios in increments of 25 %. However, we found that Cyr75 membranes had drastically different performance characteristics compared to other membranes in the series. Therefore, we also added Cyr65 and Cyr85 membranes to gauge the effects of changing bath composition around 75 % ethanol.

In addition to investigating the effects of solvent choice (Cyrene vs. GVL) and coagulation bath composition, several additional batches of membranes were fabricated to test the effect of other parameters. Cyr0-T membranes were cast into water but treated by soaking in 70 v% ethanol for 4 h immediately before testing or characterizing the membranes. Additionally, for membranes cast using GVL as the solvent, we noticed that films of dope solution were exceptionally sensitive to ambient humidity, with visible phase inversion starting to occur within only a few seconds of exposure to air of moderate (~52 %) humidity. (When using Cyrene, this occurred significantly more slowly, so there was less of a noticeable effect after 10 s.) Therefore, for "GVL" membranes, several additional batches were cast to gauge the effect of humidity on membrane morphology and performance. While most "GVL" membranes were prepared at conditions of moderate (52 ± 4 %) humidity ("-M"), we prepared two additional sets of membranes at low (26 ± 2 %) humidity ("-L").

Lastly, the performance of commercial Ultracel regenerated cellulose ultrafiltration membranes (30 kDa MWCO, "Ultracel") was tested to provide a point of comparison with our fabricated membranes. Ultracel membranes were treated to remove preservatives by soaking them in 50 v% ethanol for 30 min, followed by 25 v% ethanol for 30 min, then water for 30 min.

Table 1
Fabrication conditions for membranes.

Name	Dope solution (wt %)	Volumetric ratio of EtOH:water in coagulation bath	Other conditions/ treatments:
Cyr0	12 % PSf in Cyrene	0:100	
Cyr0-T	12 % PSf in Cyrene	0:100	Treated by soaking in 70 v % EtOH.
Cyr25	12 % PSf in Cyrene	25:75	
Cyr50	12 % PSf in Cyrene	50:50	
Cyr65	12 % PSf in Cyrene	65:35	
Cyr75	12 % PSf in Cyrene	75:25	
Cyr85	12 % PSf in Cyrene	85:15	
Cyr100	12 % PSf in Cyrene	100:0	
GVL0-M	15 % PSf in GVL	0:100	Cast at moderate humidity (52 %).
GVL25-M	15 % PSf in GVL	25:75	Cast at moderate humidity (52 %).
GVL50-M	15 % PSf in GVL	50:50	Cast at moderate humidity (52 %).
GVL75-M	15 % PSf in GVL	75:25	Cast at moderate humidity (52 %).
GVL100-M	15 % PSf in GVL	100:0	Cast at moderate humidity (52 %).
GVL50-L	15 % PSf in GVL	50:50	Cast at low humidity (26 %).
GVL75-L	15 % PSf in GVL	75:25	Cast at low humidity (26 %).
Ultracel	N/A	N/A	Treated by soaking in 50 v % EtOH, then 25 v% EtOH, then water.

2.3. Fourier transform infrared spectrometry

Fourier transform infrared spectrometry (FTIR, PerkinElmer Frontier, Waltham, MA) with attenuated total reflection (ATR) was used to detect the presence of residual solvent in membranes fabricated using different coagulation baths. After the membranes were fabricated and stored in water for 24 h, samples were cut from each batch of membranes and air-dried for 24 h before being analyzed by FTIR spectroscopy. For the "Cyr0-T" membranes, the 4 h treatment with 70 v% ethanol was done just before the air-drying step. During FTIR analysis, 4 scans were taken at 2 cm^{-1} resolution.

2.4. Scanning electron microscopy

The morphology of fabricated membranes was examined using scanning electron microscopy (SEM, FEI Nova Nanolab 200, Hillsboro, OR). To prepare top surface samples, pieces were cut from membrane sheets and air-dried. To prepare cross-sectional samples, pieces were cut

from the membrane sheets, then soaked in methanol and freeze-cracked with liquid nitrogen, then air-dried. To reduce charge buildup, samples were sputter-coated with gold using a Module Sputter Coater (SPI, West Chester, PA) before SEM imaging. Cross-sectional images were taken at 1,200x magnification and top surface images were taken at 50,000x magnification.

2.5. Contact angle measurements

Contact angle measurements were performed to gauge the hydrophilicity of fabricated membranes. Membrane samples were air-dried overnight before analysis. A contact angle instrument (Future Digital Scientific, model OCA15EC, Westbury, NY, USA) was used with a droplet size of 2 μL. For each membrane sample, a water droplet was deposited on the top surface and the contact angle was immediately measured. Measurements were taken at three locations per sample and the average angles were calculated.

2.6. Water and BSA solution filtration

Dead-end filtration experiments with water and BSA solutions were conducted using a Sterlitech HP4750 stirred cell with an effective area of 13.4 cm^2 (Fig. 1). Pressure was applied using a compressed nitrogen cylinder. Before filtration, the membranes were precompressed in a filtration cell filled with water for 2 h at 2.41 bar (35 psi). Next, water was flowed through the membranes at 2.41 bar, with 300 rpm stirring. The test was run for 50 min in total: 30 min to allow the flux to come to steady state, followed by 20 min where the water flux was acquired by tracking the weight of the permeate using an electronic balance. Flux was calculated using the following equation [44]:

$$J = \frac{Q}{(\Delta T)A}$$

where J is the permeate flux, Q is the volume permeated, ΔT is the sampling time, and A is the effective membrane area.

After the test with water was completed, another filtration test was performed under the same conditions using 1 g/L BSA solution in 10 mM phosphate buffer (pH = 7.2, prepared with sodium phosphate monobasic and sodium phosphate dibasic). Flux was also measured. From the flux values from the two tests, the flux ratio (J_{BSA}/J_{water}) was determined. BSA rejection was measured using a UV–Vis spectrophotometer (Shimadzu UV-2600i, Kyoto, Japan), based on the absorbance at 279 nm. Rejection was calculated as follows [44]:

$$R = 1 - \frac{C_p}{C_f}$$

where C_p and C_f are the concentrations of BSA in the permeate and feed, respectively.

For each membrane fabrication method, three membranes were tested and the average flux values, flux ratios, and BSA rejection percentages were calculated.

2.7. Dextran solution filtration

Dextran filtration experiments were performed to characterize the membrane rejection profile (Fig. 2). The protocol used is very similar to Wickramasinghe et al. [45]. A dextran feed solution was prepared by dissolving a blend of different molecular weight dextrans (Table 2) in 50 mM KH_2PO_4 buffer (pH = 7.0, adjusted using sodium hydroxide). Since the dextrans are polydisperse, the final mixture contains a continuous range of dextran sizes from 1 − 500 kDa. Membranes were fitted in an Amicon 50 mL stirred dead-end filtration cell (MilliporeSigma, Burlington, MA) with an effective membrane area of 13.4 cm^2. The cell was filled with dextran solution and stirred at 300 rpm. Membranes were equilibrated for 1 h under permeate recycle using a MasterFlex L/S peristaltic pump (Cole-Parmer, Vernon Hills, IL) at 0.1 mL/min flow rate. Permeate samples (1 mL each) were taken after equilibration. Three membranes were tested from several of the fabrication methods that performed best in water/BSA filtration experiments.

To determine the dextran rejection profiles, samples were analyzed using an Agilent Technologies (Santa Clara, CA) model 1260 HPLC with a refractive index detector (RID). The column used was a Shodex (New York, NY) OHpak SB-806 M HQ. The mobile phase was a 50 mM KH_2PO_4

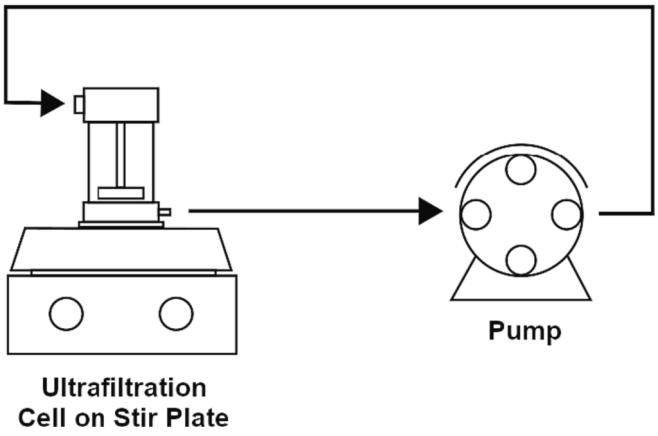

Fig. 2. Experimental setup for dextran filtration experiments.

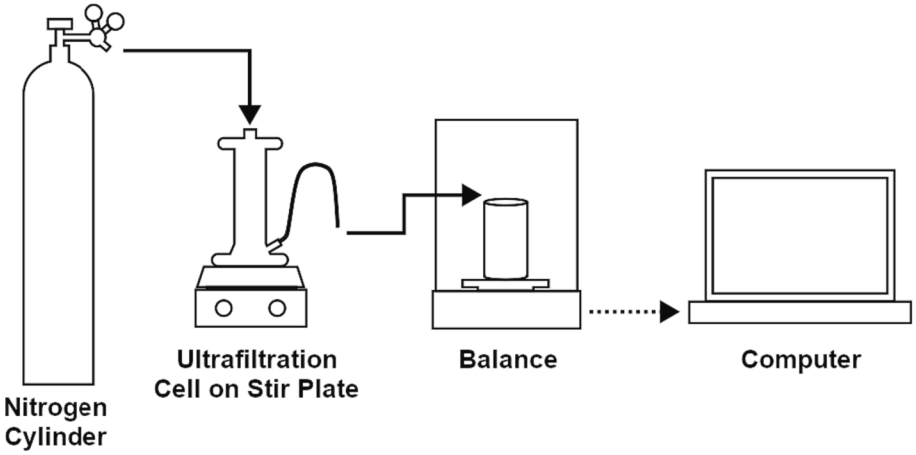

Fig. 1. Experimental setup for water flux and BSA filtration experiments.

Table 2
Dextran concentrations used in the mixed dextran feed solution.

Dextran Standard	Avg. MW (kDa)	Feed concentration (g/L)	Manufacturer
T1	1	0.74	Pharamacosmos
T4	4	1.22	Serva
T10	10	0.54	Pharamacosmos
T40	40	0.74	Pharamacosmos
T70	70	0.34	Pharamacosmos
T500	500	0.27	Pharamacosmos

buffer (pH = 7.0) with 0.5 mL/min flowrate. The sample injection volume was 10 μL and the column was operated at 25 °C. Dextran rejection profiles were calculated by comparing the HPLC chromatograms of feed and permeate samples (details given in section S2 of the supplementary information). The MWCO of each membrane was calculated based on the smallest dextran size that was at least 90 % rejected.

2.8. Cloud point measurements

Cloud point measurements were performed by first dissolving various concentrations of PSf in solvent (Cyrene or GVL). The solutions prepared were 2.5, 5, 7.5, 10, and 12 wt% PSf in Cyrene, and 2.5, 5, 7.5, 10, 12.5, and 15 wt% PSf in GVL. Next, nonsolvent (water or ethanol) was gradually pipetted into the solution under stirring at room temperature. The test was stopped when the solution became visibly cloudy and remained cloudy after 1 h of stirring.

3. Results

3.1. Cloud point measurements

Cloud point experiments were performed, where water or ethanol was gradually pipetted into PSf/Cyrene and PSf/GVL solutions until the solution became cloudy, indicating that phase inversion had occurred. The results show that water is a very strong nonsolvent for the PSf/Cyrene system (Fig. 3a) since phase inversion occurred when water comprised < 0.4 wt% of the mixture. Ethanol was a much weaker nonsolvent – phase inversion occurred at 11–13 wt% ethanol. For the PSf/GVL solution (Fig. 3b), water was an extremely strong nonsolvent, with minimal water required to cause phase inversion. For dilute solutions, phase inversion occurred after the addition of < 0.1 wt% water. Ethanol was also a strong nonsolvent for the PSf/GVL solution, although not as strong as water.

3.2. Fourier transform infrared spectrometry

Samples of fabricated membranes were analyzed by FTIR (Fig. 4, full spectrums in supplementary information section S3). Since PSf does not have carbonyl groups, while Cyrene and GVL do have carbonyl groups, membrane spectra were examined for distinctive carbonyl peaks in the 1700–1800 cm^{-1} range to determine whether residual solvent remained in the membranes. Dual peaks around 1724 and 1740 cm^{-1} are characteristic of the carbonyl group in Cyrene [46], while a peak at around 1766 cm^{-1} is characteristic of the carbonyl group in GVL [47]. For the Cyr0 and GVL0-M membranes, there were clear signals of residual solvent (Fig. 4a). This was indicated by carbonyl peaks at 1726 and 1743 cm^{-1} from Cyrene in the Cyr0 spectrum, and a peak at 1772 cm^{-1} from GVL in the GVL0-M spectrum.

For membranes cast using Cyrene as the solvent (Fig. 4b), the peaks for residual Cyrene vanished in the FTIR spectrum of the Cyr0-T membrane. Cyr25 – Cyr100 membranes had reduced peak signal compared to Cyr0 membranes, with the Cyr65 sample having the shortest peaks. This indicates that ethanol/water mixtures, especially around 65 % ethanol, were more effective at removing residual Cyrene than pure water. For membranes cast using GVL as the solvent (Fig. 4c), the peak for residual GVL was highest for the GVL0-M membrane and fell with increasing concentrations of ethanol in the coagulation bath. This shows that coagulation baths with relatively high concentrations of ethanol were more effective at removing residual GVL than the water coagulation bath.

3.3. Scanning electron microscopy

Cross sections and top surfaces of membranes were imaged using SEM (Fig. 5). Additional SEM images, including enlarged cross-sectional images, are provided in supplementary information section S4. All membranes had sponge-like morphologies. However, aspects of membrane morphology such as pore size and surface texture varied substantially depending on fabrication conditions.

Cyr0 membranes had wrinkled surfaces with large crevasses. Very few circular pores were visible on the surface. Meanwhile, the cross-sectional image showed that the polymer-poor domains were largest in the middle of the membrane and smaller near the top and bottom.

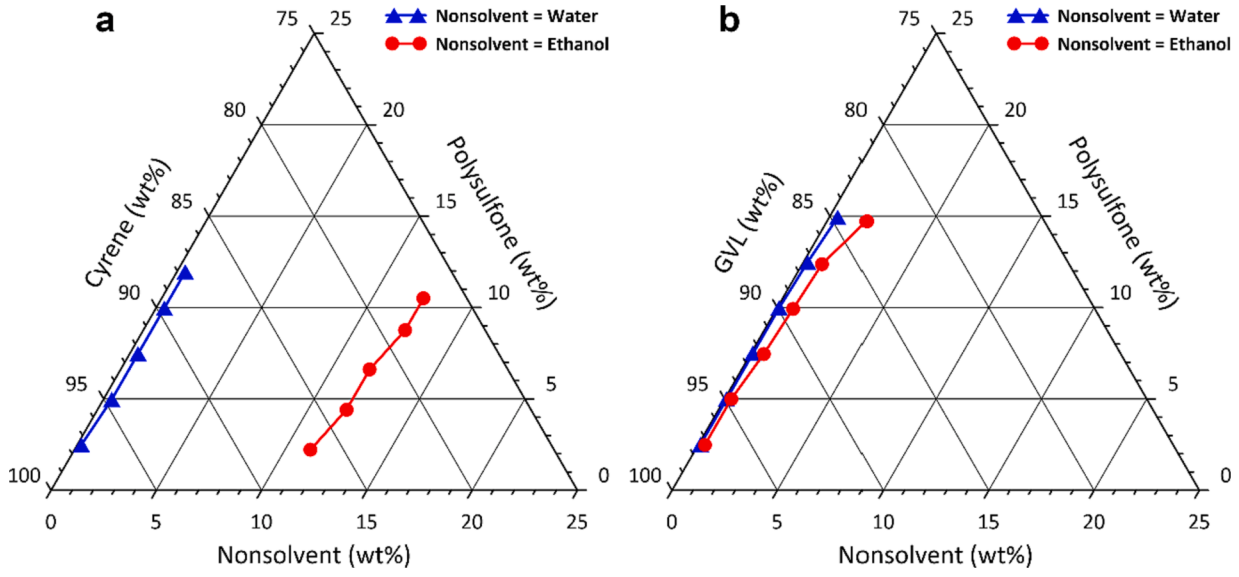

Fig. 3. Ternary phase diagrams of polysulfone/solvent/nonsolvent systems with: (a) Cyrene as the solvent and (b) GVL as the solvent.

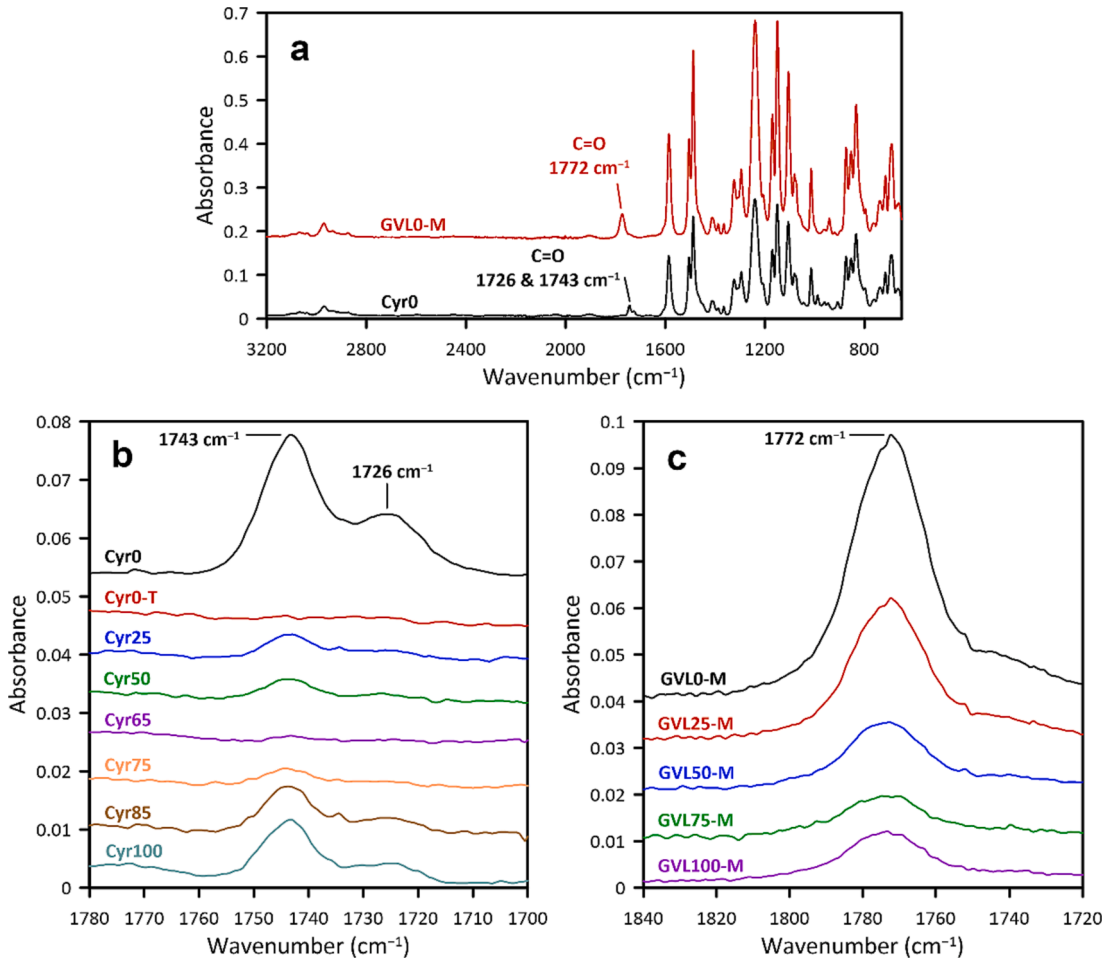

Fig. 4. FTIR spectra for: (a) Cyr0 and GVL0-M membranes, showing the locations of peaks for residual Cyrene at 1726 and 1743 cm^{-1} and residual GVL at 1772 cm^{-1}. (b) Detail of Cyr membrane spectra at the locations of the Cyrene peaks. (c) Detail of GVL membrane spectra at the location of the GVL peak.

These features can be explained by the slow and limited mixing between Cyrene and water (analyzed more fully in the discussion). Residual Cyrene remained trapped near the middle of the membrane, with water slowly diffusing inward. This allowed polymer-poor domains near the middle to coalesce and grow. Although the top surface solidified quickly, phase separation was delayed for the lower layers of the membrane, which provided time for the top surface to shift and crumple.

Cyr25 and Cyr50 membranes also had larger domains near the middle than near the top and bottom. The top surfaces were rough, with few visible pores. The Cyr25 and Cyr50 membranes did not have the large wrinkles and crevasses present in the Cyr0 membranes. This was likely due to better miscibility between Cyrene and the ethanol/water mixtures in the coagulation baths.

Cyr65 and Cyr75 membranes had typical asymmetric pore morphologies, with small pores near the top surface and pore size increasing with depth. These morphologies, combined with the FTIR results, indicate that the mixed ethanol/water coagulation baths were able to induce fast demixing and readily remove Cyrene from the membranes. Both Cyr65 and Cyr75 membranes had flat, porous top surfaces. Pores were slightly larger for Cyr75 membranes than for Cyr65 membranes.

Cyr85 and Cyr100 membranes both had rough, nodular surface morphologies. Cyr100 membranes also had a unique cross-sectional morphology. The domains were very large, indicating that the domains had a long time to grow before solidifying. There was also a thick, apparently impermeable, top layer. This can be explained by ethanol's relative weakness as a nonsolvent. Ethanol was unable to induce fast demixing and produce a porous selective layer.

GVL0-M, GVL25-M, GVL50-M, and GVL75-M membranes (cast at moderate humidity) all had asymmetric sponge-like morphologies. GVL0-M membranes had very few pores on the top surface. This is consistent with poor mixing between GVL and water, which did not allow for many pores to be formed. GVL50-M and GVL75-M membranes had much higher densities of pores on their surfaces, as mixtures of water and ethanol removed GVL from the films more effectively. Interestingly, all of these membranes had top surfaces covered with dimples ~ 1 μm wide. The dimples can be explained by breath-figure self-assembly [48]. This is a process where a film of polymer solution is exposed to water vapor, which condenses into droplets at the surface of the film. The water droplets act as a template, forming pores or dimples in the polymer solution. Typically, in breath-figure self-assembly, the polymer solidifies after evaporation of the water droplets and solvent. However, in this case, solidification occurs due to NIPS.

GVL100-M membranes had a morphology similar to Cyr100 membranes: larger domains were visible in the cross section and membranes had a relatively nonporous top surface. This can again be explained by delayed demixing, as ethanol is a relatively weak nonsolvent.

GVL50-L and GVL75-L membranes (both cast at low humidity) had surface morphologies very different from membranes cast at moderate humidity. For GVL50-L and GVL75-L membranes, there was a high density of pores on the surfaces, and the pores were large. Additionally, the surfaces were flat, without dimples. In this case, the humidity was too low to allow for breath-figure self-assembly. The effects of humidity will be explored more in the discussion.

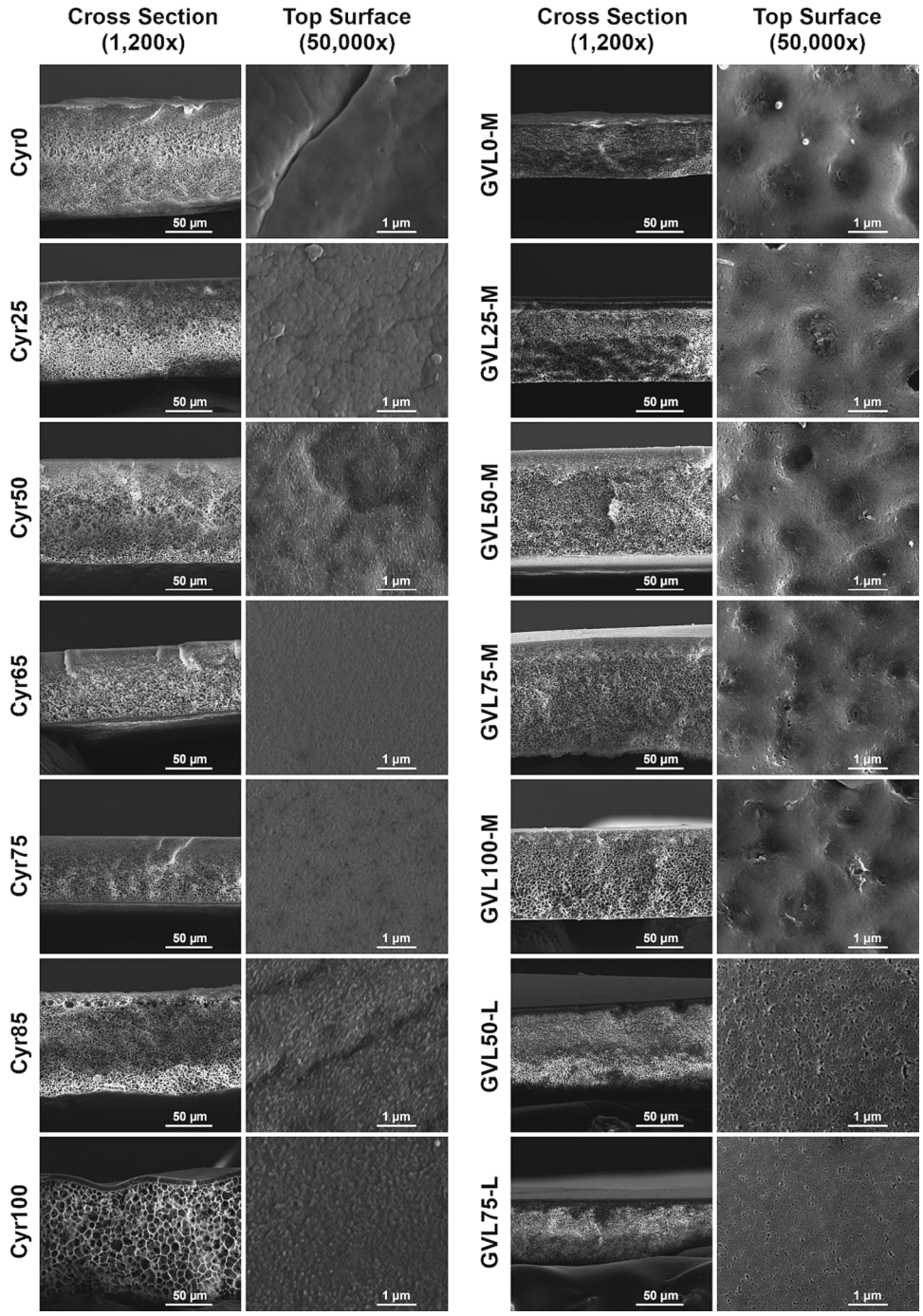

Fig. 5. SEM images of cross sections and top surfaces of membranes.

3.4. Contact angle measurements

Contact angle measurements (Fig. 6) showed small variation between membranes, ranging from Cyr85 on the low end, with a water contact angle of 55.1 ± 2.3°, to GVL100-M on the high end, with a water contact angle of 76.2 ± 10.1°. Since all membranes were made from PSf and no surface modifications were added, the relatively narrow range of contact angles is not surprising. Still, a few notable observations can be made. First, Cyr0 membranes had a contact angle (66.9 ± 1.3°) virtually identical to Cyr0-T membranes (67.9 ± 1.2°), which indicates that the treatment with 70 % ethanol did not affect the membranes' hydrophilicity. Also, Cyr85 and Cyr100 membranes had the lowest contact angles, which is consistent with their rough, nodular surface texture observed in SEM images. Surface roughness increases wetting of materials if a smooth surface of the same material has a contact angle $< 90°$ [49]. Lastly, for membranes cast using GVL, low humidity generally led to lower contact angles. For instance, the contact angle for GVL50-L membranes was 63.1 ± 1.0°, substantially lower than the contact angle for GVL50-M membranes, 74.6 ± 2.9°. This is likely caused by the more porous surface of GVL50-L (visible when comparing SEM images), since higher porosity allows for more liquid penetration, lowering the contact angle [49].

3.5. Water and BSA solution filtration

Dead-end filtration was performed by filtering water and BSA

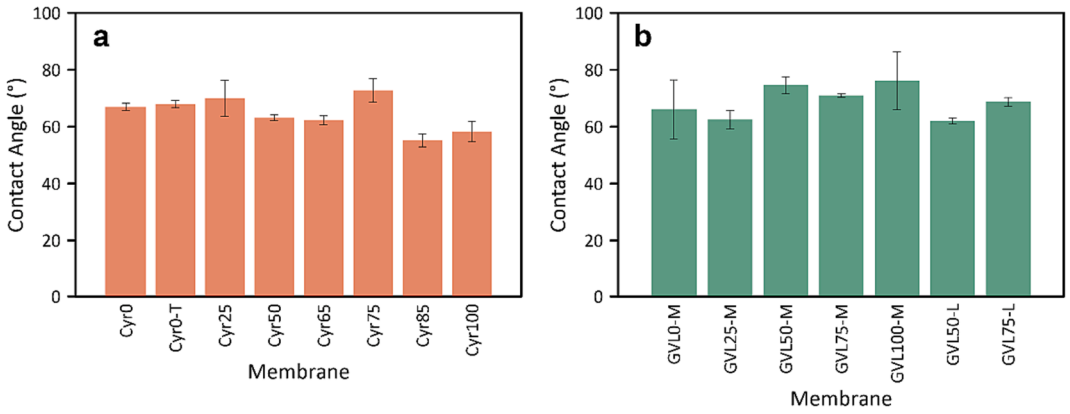

Fig. 6. Water contact angles of membranes fabricated from (a) Cyrene and (b) GVL.

solutions through the membranes (Fig. 7). For membranes cast using Cyrene, the amount of ethanol in the coagulation bath significantly influenced flux and BSA rejection. Cyr0 membranes had a water flux of 63.4 ± 17.4 LMH and a low BSA rejection of only 12.7 ± 11.5 %. Cyr0-T membranes had very close flux and rejection values, indicating that even though the treatment with 70 v% ethanol removed residual Cyrene, it had no significant effect on membrane performance. The low BSA rejection is likely due to the BSA passing through the large crevasses that were visible in the SEM images. Cyr25, Cyr50, and Cyr100 membranes had very low or zero flux. This is consistent with the lack of pores visible on the top surfaces in the SEM images of each of these membranes. Due to the near-zero flux, it was not possible to collect BSA permeate samples and measure rejection for these membranes. Cyr65 and Cyr75 membranes had the best overall performance. Cyr65 membranes had a water flux of 70.1 ± 19.5 LMH and BSA rejection of 96.7 ± 1.6 %. Cyr75 membranes had a water flux of 140.4 ± 55.0 LMH and BSA rejection of 85.6 ± 6.8 %.

Among the GVL membranes, those cast into pure water (GVL0-M) and pure ethanol (GVL100-M) were both impermeable. However, membranes cast into mixtures of water and ethanol had improved flux. Water flux was highest for the GVL75-L membranes, at 268.6 ± 32.1 LMH, although these membranes had low BSA rejection, 23.5 ± 14.5 %. BSA rejection was highest for GVL50-M membranes, which had a water flux of 37.6 ± 4.6 LMH and a BSA rejection of 92.7 ± 1.8 %. Comparing membranes cast at different humidity levels, membranes cast at low humidity had much higher fluxes and much lower rejections than those cast at moderate humidity. This is consistent with the SEM images showing larger pores on the surface for those cast at low humidity.

One additional trend is that membranes cast from GVL generally had a higher flux ratio (i.e. less flux decline during the BSA filtration vs. water filtration), compared to membranes cast from Cyrene. For example, comparing the two membrane types with the highest BSA rejection, GVL50-M membranes had a flux ratio of 0.704 ± 0.033, while for Cyr65 membranes it was only 0.362 ± 0.074. In practice, this meant that while Cyr65 membranes had a water flux nearly twice as high as GVL50-M membranes (70.1 ± 19.5 vs. 37.6 ± 4.6 LMH), their fluxes during BSA filtration were virtually the same (26.1 ± 10.8 vs. 26.5 ± 4.1 LMH).

Lastly, Ultracel membranes had a water flux of 398.0 ± 69.1, BSA flux of 93.7 ± 1.7, and BSA rejection of 98.3 ± 1.1 %. These flux and rejection values were higher than the membranes prepared using Cyrene and GVL, although the flux ratio was relatively low at 0.241 ± 0.044.

The filtration performance of membranes fabricated here was compared to the performance of PSf membranes fabricated from traditional solvents (DMAc, DMF, and NMP) from the literature (Table 3, [50–52]). Membranes with at least 90 % BSA rejection were selected. To maintain an even comparison, only data on membranes fabricated using a dope solution of PSf/solvent without additives were included. Cyr65 and GVL50-M membranes generally had filtration performance competitive with those cast using traditional solvents, although one set of membranes made using DMF [52] and one set made using NMP had moderately higher permeability [53].

3.6. Dextran solution filtration

Dead-end filtration was performed using dextran solutions on four sets of membranes (Cyr65, Cyr75, GVL50-M, and GVL75-M) that had good overall performance during dead-end filtration with water and BSA solution. Additionally, Ultracel membranes were tested as a point of comparison. Dextran rejection curves were plotted based on the results (Fig. 8).

For most of the batches of fabricated membranes, there was significant variability in the rejection curves among the three membranes tested. This is likely because membranes were fabricated by hand, so it was difficult to precisely control all the variables (i.e. blade draw speed, air exposure time, etc.) in order to ensure uniformity between membranes. Better consistency could likely be achieved by using automated casting equipment. The rejection profiles of the three Ultracel membranes were very similar, which indicates that the likely source of the variability seen with other membranes is in the fabrication step and not the dextran filtration tests. Still, there were clear trends in results between different types of membranes.

Cyr65 membranes had much lower MWCOs (21.3–42.2 kDa) than Cyr75 membranes (93.3–177.3 kDa). This is consistent with the smaller pore sizes observed in surface SEM images of the Cyr65 membrane and the higher BSA rejection for the Cyr65 membranes, relative to Cyr75 membranes. GVL50-M membranes had MWCOs of 70.9–78.9 kDa, which was a narrower range than GVL75-M membranes, which had MWCOs ranging from 66.0 to 118.7 kDa. These results are also consistent with GVL50-M membranes having higher BSA rejection than the GVL75-M membranes. The Ultracel membranes had minimal variability, with MWCOs ranging from 38.4 to 45.8 kDa. Also, Ultracel membranes had noticeably sharper rejection profiles than our fabricated membranes.

4. Discussion

4.1. Significance of Hansen solubility parameters

Differing interactions between polymer, solvent, and nonsolvent play an important role in explaining many of the experimental results above. Hansen solubility parameters are commonly used to describe the ability of various solvents to dissolve polymers [54]. Three solubility parameters – δ_d, δ_p, and δ_h – are used to quantify the dissipative, polar, and hydrogen bonding interactions, respectively. Polymers generally dissolve in solvents that have similar solubility parameters to the

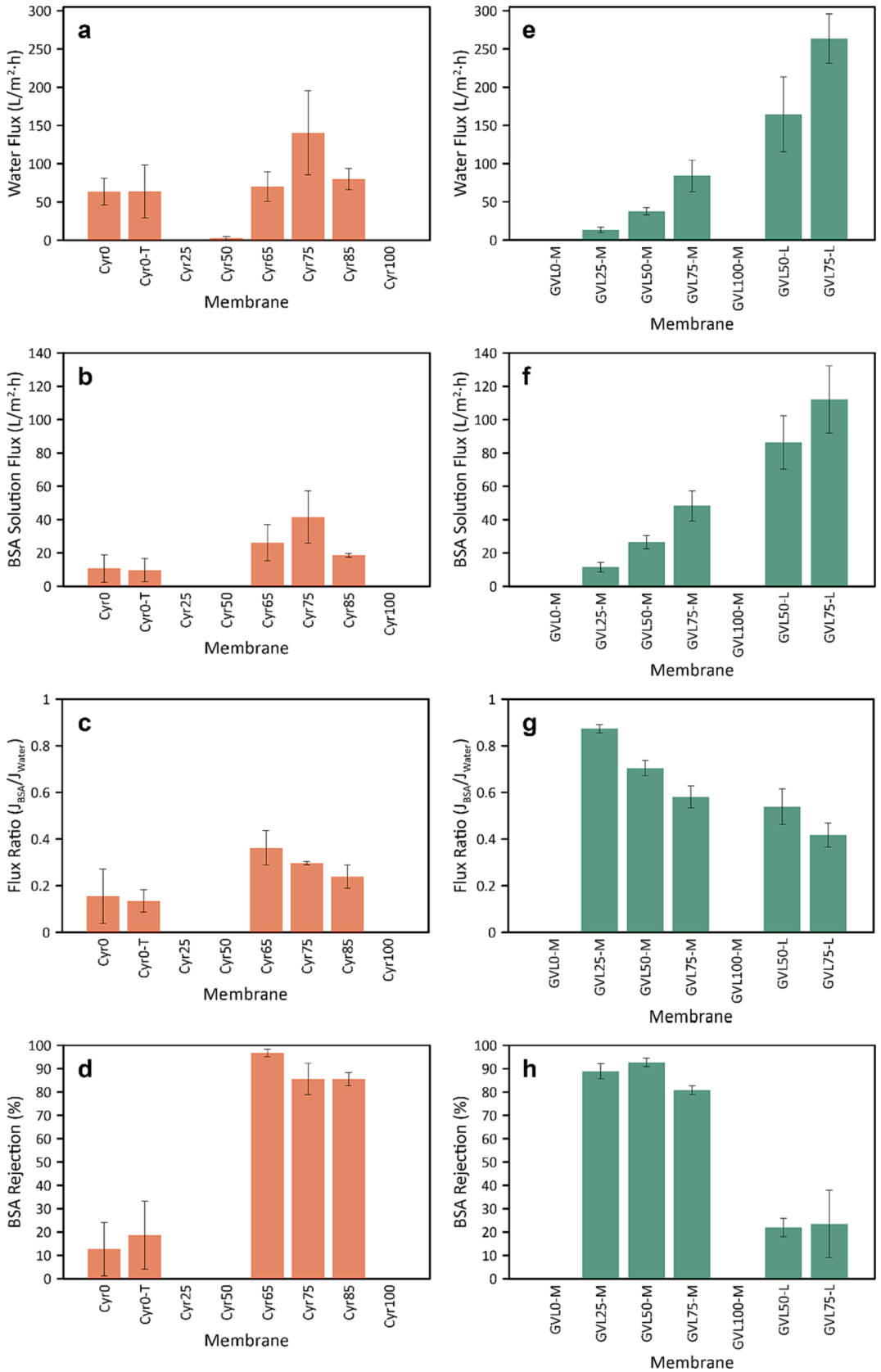

Fig. 7. Flux and BSA rejection data for (a-d) membranes cast using Cyrene and (e-h) membranes cast using GVL. Membranes without bars shown had zero flux during filtration with water or BSA solution.

Table 3
Comparison of flux and BSA rejection with PSf membranes made from traditional solvents.

Polymer	Solvent	Polymer wt%	Pressure (bar)	Water flux (LMH)	Permeability (LMH/bar)	BSA rejection (%)	Source
PSf	Cyrene	12	2.41	70.1	29.1	96.7	This study (Cyr65)
PSf	GVL	15	2.41	37.6	15.6	92.7	This study (GVL50-M)
PSf	DMAc	17.5	3.45	36.8	10.7	90.1	[50]
PSf	DMF	17.5	3.45	11.2	3.2	95.1	[50]
PSf	DMAc	17	4.00	63.0	15.8	96.0	[51]
PSf	DMF	16	2.00	111.5	55.8	95.2	[52]
PSf	NMP	15	3.00	139.0	46.3	>96.0 %	[53]

polymer.

Chemical properties, including Hansen solubility parameters for the polymer, solvents, and nonsolvents used in this study, are shown in Table 4. The Hansen solubility parameters explain several trends that were observed in the cloud point data. Water was a very strong nonsolvent for both dope solutions, as its δ_h value, 42.3, is much higher than PSf's δ_h value of 7.1. Therefore, minimal amounts of water must be added to the dope solution to cause PSf to become insoluble. Ethanol was not as strong a nonsolvent since its δ_h value, 19.4, was markedly lower than that of water.

Additionally, PSf/GVL dope solutions were more sensitive to the addition of nonsolvents than PSf/Cyrene dope solutions. This is likely explained by the fact that Cyrene has solubility parameters very close to those of PSf, while GVL has solubility parameters somewhat further away from PSf (especially for the δ_p parameter, which was 14.0 for GVL and 8.2 for PSf). Therefore, PSf is less stable in GVL than in Cyrene.

4.2. Effect of coagulation bath composition

When membranes were cast using pure water in the coagulation bath, substantial amounts of residual solvent (whether Cyrene or GVL) remained trapped in the membranes. This is explained by the relatively poor compatibility between these two solvents and water. Although both Cyrene and GVL are reported to be miscible in water [10,57], there is a large difference between the δ_h values of Cyrene (6.9) and GVL (8.0) compared to the δ_h value of water (42.3). This difference in the strength of hydrogen bonding seems to limit the speed of mixing between the solvents and water. For example, Mohsenpour et al. found that water and Cyrene remained in distinct phases after 48 h of contact when there was no agitation [22].

Addition of ethanol to the coagulation bath resolved the problem of poor miscibility. When ethanol was added, it increased the hydrophobicity of the nonsolvent phase, allowing Cyrene and GVL to mix with the nonsolvent and diffuse out of the film into the coagulation bath more easily. Hence, less residual solvent remained in the membranes and a higher density of pores was formed on the surface.

On the other hand, we found that use of pure ethanol in the coagulation bath resulted in impermeable membranes. Cloud point data suggests that this is because ethanol is too weak of a nonsolvent to quickly induce phase inversion. During phase inversion, the delayed demixing led to the formation of membranes with relatively dense top surfaces. Thus, pure ethanol should not be used in the coagulation bath. Rather, a balance should be struck between the high miscibility of ethanol with Cyrene/GVL, and the high nonsolvent strength of water. Here, we tested a range of ethanol:water compositions to find the optimal balance. Coagulation bath compositions of 50:50–75:25 volumetric ratio ethanol: water were best able to strike the balance between miscibility and nonsolvent strength, resulting in good pore formation.

Additionally, we found that Cyr0-T membranes, which were cast into pure water during the fabrication process, then treated with 70 v% ethanol later, did not have improved dead-end filtration performance compared with Cyr0 membranes. This shows that it is important to ensure that solvent is effectively removed during the NIPS process itself, when pore formation occurs, as opposed to during a post-treatment step later.

4.3. Effect of humidity

The sensitivity of "GVL" membranes to humidity is explained by the extremely high nonsolvent strength of water towards the PSf/GVL dope solution. Exposure of the film to moderate humidity levels for even a few seconds begins to cause phase inversion on the surface of the film. Hence, a relatively dense surface layer forms on the top surface of the "-M" membranes before they are submerged in the coagulation bath. This leads to smaller pores and higher BSA rejection for these membranes, relative to the "-L" membranes (Fig. 9).

Additionally, exposure to moderate humidity led to the formation of dimples on "-M" membranes. Dead-end filtration results indicate possible antifouling effects of these dimples. Dimpled membranes generally had less flux decline (higher flux ratios) than "Cyr" membranes during dead-end filtration tests with BSA. Little work has been done to specifically investigate antifouling effects of dimples on filtration membranes. However, research has found that micropatterning on membranes can induce shear stresses as water flows across the surface, which promotes mixing and reduces deposition of foulants [58–60].

4.4. Sustainable processing

As discussed in the introduction, Cyrene and GVL have reduced toxicity compared to traditional solvents such as NMP, DMF, and DMAc. However, the use of ethanol/water mixtures in the coagulation bath could create additional safety issues since ethanol is flammable. The flash point of pure ethanol is 12.7 °C, while the flash point of ethanol/water mixtures varies depending on concentration – for example, the flash point is 23 °C for a mixture of 59 v% ethanol in water [61]. Thus, while the toxicity of the solvents is reduced, flammability is a concern.

Although ethanol is flammable, some rankings of chemicals still place it as less hazardous than solvents such as NMP, DMAc, and DMF. For example, Prat et al. [62], evaluated 51 solvents based on their health, safety, and environmental hazards, as given by several solvent selection guides. Solvents were ranked into four categories: recommended, problematic, hazardous, and highly hazardous. Ethanol was ranked in the most favorable category, "recommended", while NMP, DMAc, and DMF were in the second least-favorable category, "hazardous". Thus, the risks associated with ethanol/water mixtures may be preferable to the risks associated with NMP, DMAc, and DMF, at least in some applications.

This work suggests that use of the values of the Hansen solubility parameters for mixtures of ethanol and water that were successfully used in this study could provide a "target" for screening other nonsolvents. This could not only provide a more rational way to select nonsolvent mixtures for optimizing membrane morphology but also a way to survey alternatives to ethanol that are less flammable.

Though membrane-based separations are often claimed to be much more sustainable than competing technologies such as distillation, membrane manufacturing processes use highly toxic, environmentally unfriendly chemicals that are not sustainable. There is a great need to switch to green solvents. However, given the complicated dependence of

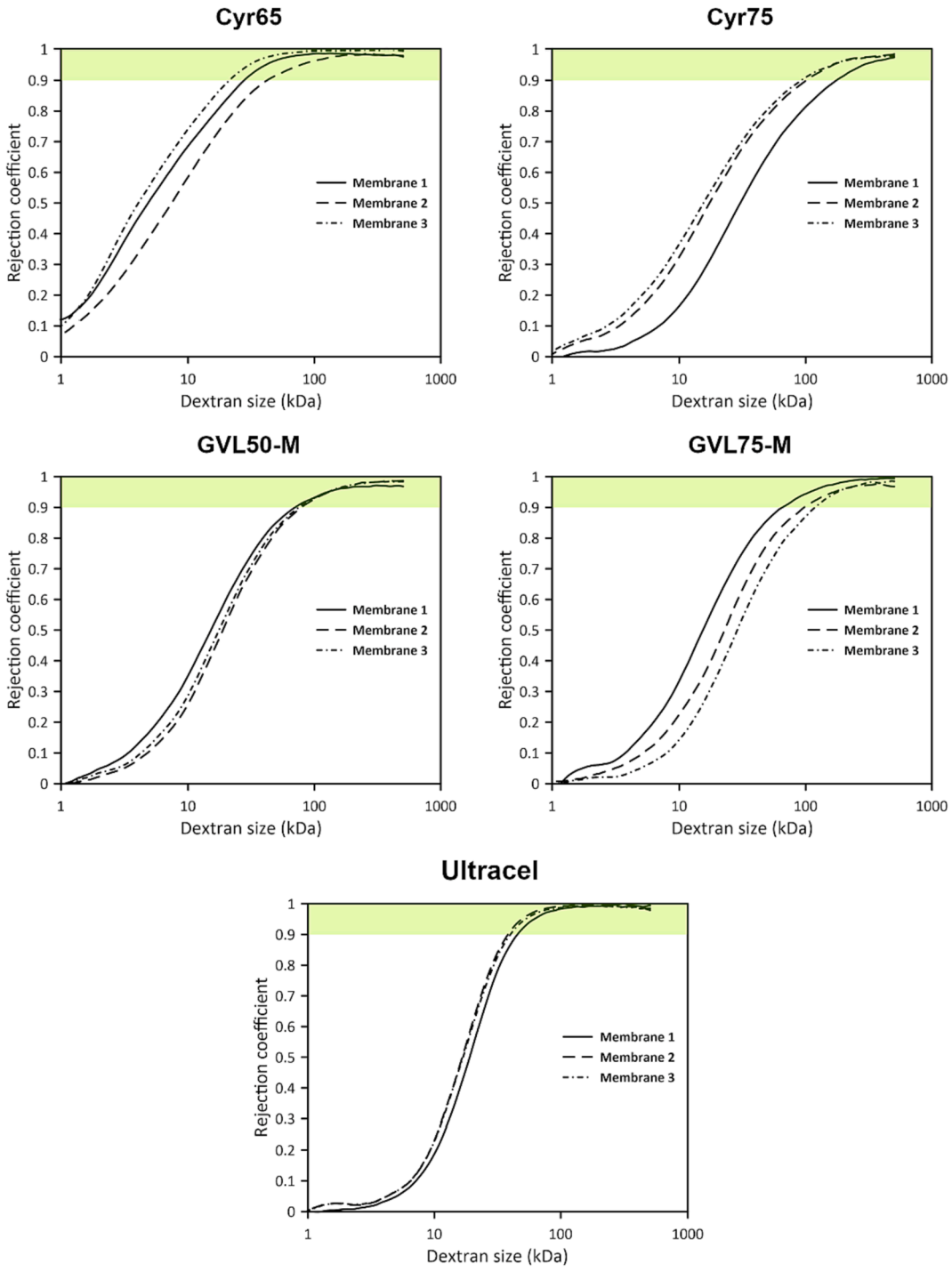

Fig. 8. Rejection coefficients of dextrans (1–500 kDa) for Cyr65, Cyr75, GVL50-M, GVL75-M, and Ultracel membranes. Three membranes were tested per fabrication method. MWCO was calculated based on the smallest dextran size that was at least 90 % rejected (light green shading). (For interpretation of the references to colour in this figure legend, the reader is referred to the web version of this article.)

membrane properties on the casting conditions, solvents and additives, replacement of current solvents will be challenging. Here we show that by using values of the Hansen solubility parameters combined with membrane characterization one can identify likely replacement solvents and solvent mixtures for phase inversion membrane casting.

5. Conclusions

In this study, PSf UF membranes were fabricated using the green solvents, Cyrene and GVL. The effects of coagulation bath composition on membrane characteristics were investigated. The following conclusions can be drawn:

- Either Cyrene or GVL can be used as solvents for fabricating PSf UF membranes.
- For both solvents, (Cyrene and GVL,) the coagulation bath composition plays a significant role in shaping membrane properties. Use of mixed nonsolvents in the coagulation bath provides more flexibility to optimize membrane morphology and hence performance.

Table 4
Chemical properties of polymer, solvents, and nonsolvents used [15,17,27,55,56].

Chemical	Structure	δ_d ($MPa^{1/2}$)	δ_p ($MPa^{1/2}$)	δ_h ($MPa^{1/2}$)	Density (g/cm^3)	Viscosity (cP)
PSf	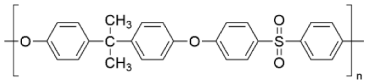	18.5	8.2	7.1	1.24	N/A
Cyrene	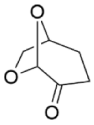	18.8	10.6	6.9	1.25	14.5
GVL	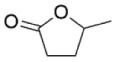	16.7	14.0	8.0	1.05	2.2
Water		15.5	16	42.3	1.00	1.0
Ethanol		15.8	8.8	19.4	0.79	1.1

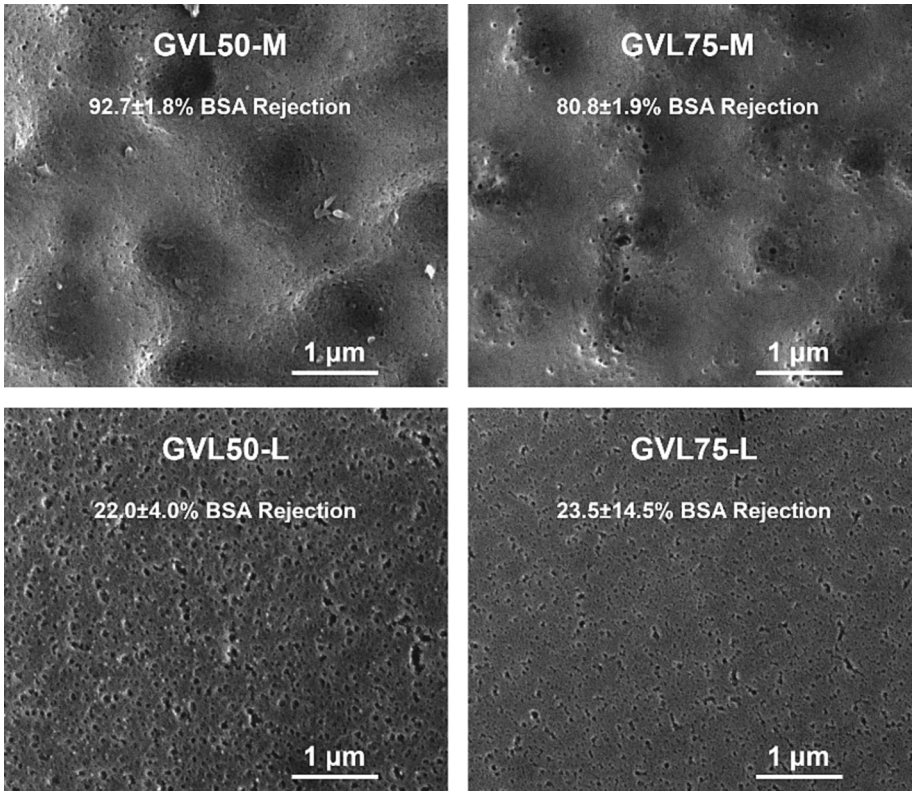

Fig. 9. Comparison of top surface SEM images and BSA rejections of GVL50-M, GVL75-M, GVL50-L, and GVL75-L membranes.

- When water was used in the coagulation bath, substantial residual solvent remained trapped in the membranes due to poor mixing between the solvents and water. Additionally, the resulting membranes were either impermeable or had very low BSA rejection.
- Using mixtures of ethanol and water (50:50–75:25 volumetric ratio) in the coagulation bath removed more residual solvent from the membranes than when water alone was used. Using mixtures of ethanol and water also improved pore formation, resulting in membranes with higher flux and rejection.
- Humidity had a drastic effect on the morphology of membranes cast using GVL. Brief exposure to moderate (52 %) humidity resulted in membranes with much smaller pores than membranes cast at low (26 %) humidity. Membranes fabricated under moderate humidity also had novel ~ 1 μm surface dimples and relatively little flux decline during BSA filtration.
- The use of parameters such as the Hansen solubility parameters combined with performance data will be essential to rapidly identify optimal membrane casting conditions.

CRediT authorship contribution statement

Cannon Hackett: Formal analysis, Investigation, Methodology, Writing – original draft. **David Hale:** Investigation. **Brianna Bair:** Investigation. **God's-Delight Manson-Endeboh:** Investigation. **Xiaolei Hao:** Investigation. **Xianghong Qian:** Methodology, Supervision. **S. Ranil Wickramasinghe:** Methodology, Supervision, Writing – review &

editing. **Audie Thompson:** Methodology, Supervision, Writing – review & editing.

Declaration of Competing Interest

The authors declare that they have no known competing financial interests or personal relationships that could have appeared to influence the work reported in this paper.

Data availability

Data will be made available on request.

Acknowledgements

Norafiqah Ismail is thanked for her suggestions regarding membrane fabrication.

Funding

Funding was provided by the National Science Foundation Division of Engineering Education and Centers, Research Experiences for Undergraduates, 2150436, and the Membrane Science, Engineering and Technology Center through the National Science Foundation Division of Emerging Frontiers & Multidisciplinary Activities, 2207153. Funding for equipment used in this research was provided by the Center for Advanced Surface Engineering, under the National Science Foundation Grant No. OIA -1457888 and the Arkansas EPSCoR Program, ASSET III.

Appendix A. Supplementary material

Supplementary data to this article can be found online at https://doi.org/10.1016/j.seppur.2023.125752.

References

[1] M. Mulder, Basic Principles of Membrane Technology, 2nd ed., Kluwer Academic Publishers, 1996.
[2] A.M. Nasir, M.R. Adam, S.N.E.A. Mohamad Kamal, J. Jaafar, M.H.D. Othman, A. F. Ismail, F. Aziz, N. Yusof, M.R. Bilad, R. Mohamud, M.A. Rahman, W.N. Wan Salleh, A review of the potential of conventional and advanced membrane technology in the removal of pathogens from wastewater, Sep. Purif. Technol. 286 (2022), 120454, https://doi.org/10.1016/j.seppur.2022.120454.
[3] N. Hampu, J.R. Werber, W.Y. Chan, E.C. Feinberg, M.A. Hillmyer, Next-generation ultrafiltration membranes enabled by block polymers, ACS Nano 14 (2020) 16446–16471, https://doi.org/10.1021/acsnano.0c07883.
[4] G.R. Guillen, Y. Pan, M. Li, E.M.V. Hoek, Preparation and characterization of membranes formed by nonsolvent induced phase separation: a review, Ind. Eng. Chem. Res. 50 (2011) 3798–3817, https://doi.org/10.1021/ie101928r.
[5] U. Hass, S.P. Lund, J. Elsner, Effects of prenatal exposure to N-methylpyrrolidone on postnatal development and behavior in rats, Neurotoxicol. Teratol. 16 (1994) 241–249, https://doi.org/10.1016/0892-0362(94)90045-0.
[6] K. Sitarek, J. Stetkiewicz, Assessment of reproductive toxicity and gonadotoxic potential of N-methyl-2-pyrrolidone in male rats, Int. J. Occup. Med. Environ. Health 21 (2008), https://doi.org/10.2478/v10001-008-0006-z.
[7] G.L. Kennedy, Acute and subchronic toxicity of dimethylformam ide and dimethylacetamide following various routes of administration, drug and chemical, Toxicology 9 (1986) 147–170, https://doi.org/10.3109/01480548608998272.
[8] G.L. Kennedy, Toxicology of dimethyl and monomethyl derivatives of acetamide and formamide: a second update, Crit. Rev. Toxicol. 42 (2012) 793–826, https://doi.org/10.3109/10408444.2012.725028.
[9] P.A. Fail, J.D. George, T.B. Grizzle, J.J. Heindel, Formamide and dimethylformamide: reproductive assessment by continuous breeding in mice, Reprod. Toxicol. 12 (1998) 317–332, https://doi.org/10.1016/S0890-6238(98)00011-2.
[10] F. Prézélus, J.-C. Remigy, C. Guigui, L. Tiruta-Barna, Does substituting reprotoxic solvents during ultrafiltration membrane fabrication really mitigate environmental impacts? Focus on drinking water production, J. Clean. Prod. 337 (2022), 130476, https://doi.org/10.1016/j.jclepro.2022.130476.
[11] n-Methylpyrrolidone (NMP); Revision to Toxic Substances Control Act (TSCA) Risk Determination; Notice of Availability, Federal Register. (2022). https://www.federalregister.gov/documents/2022/12/19/2022-27438/n-methylpyrrolidone-nmp-revision-to-toxic-substances-control-act-tsca-risk-determination-notice-of (accessed June 2, 2023).
[12] M. Razali, J.F. Kim, M. Attfield, P.M. Budd, E. Drioli, Y.M. Lee, G. Szekely, Sustainable wastewater treatment and recycling in membrane manufacturing, Green Chem. 17 (2015) 5196–5205, https://doi.org/10.1039/C5GC01937K.
[13] S.A. Naziri Mehrabani, V. Vatanpour, I. Koyuncu, Green solvents in polymeric membrane fabrication: a review, Sep. Purif. Technol. 298 (2022), 121691, https://doi.org/10.1016/j.seppur.2022.121691.
[14] J. Sherwood, M.D. Bruyn, A. Constantinou, L. Moity, C.R. McElroy, T.J. Farmer, T. Duncan, W. Raverty, A.J. Hunt, J.H. Clark, Dihydrolevoglucosenone (Cyrene) as a bio-based alternative for dipolar aprotic solvents, Chem. Commun. 50 (2014) 9650–9652, https://doi.org/10.1039/C4CC04133J.
[15] H.J. Salavagione, J. Sherwood, M.D. Bruyn, V.L. Budarin, G.J. Ellis, J.H. Clark, P. S. Shuttleworth, Identification of high performance solvents for the sustainable processing of graphene, Green Chem. 19 (2017) 2550–2560, https://doi.org/10.1039/C7GC00112F.
[16] J.R. Langan, G.A. Salmon, Physical properties of N-methylpyrrolidinone as functions of temperature, J. Chem. Eng. Data. 32 (1987) 420–422, https://doi.org/10.1021/je00050a009.
[17] A.T. Bridge, B.J. Pedretti, J.F. Brennecke, B.D. Freeman, Preparation of defect-free asymmetric gas separation membranes with dihydrolevoglucosenone (CyreneTM) as a greener polar aprotic solvent, J. Membr. Sci. 644 (2022), 120173, https://doi.org/10.1016/j.memsci.2021.120173.
[18] Y.X. Foong, L.H. Yew, P.V. Chai, Green approaches to polysulfone based membrane preparation via dimethyl sulfoxide and eco-friendly natural additive gum Arabic, Mater. Today:. Proc. 46 (2021) 2092–2097, https://doi.org/10.1016/j.matpr.2021.04.470.
[19] R.A. Milescu, A. Zhenova, M. Vastano, R. Gammons, S. Lin, C.H. Lau, J.H. Clark, C. R. McElroy, A. Pellis, Polymer chemistry applications of cyrene and its derivative cygnet 0.0 as safer replacements for polar aprotic solvents, ChemSusChem 14 (2021) 3367–3381, https://doi.org/10.1002/cssc.202101125.
[20] T. Marino, F. Galiano, A. Molino, A. Figoli, New frontiers in sustainable membrane preparation: Cyrene^{TM} as green bioderived solvent, J. Membr. Sci. 580 (2019) 224–234, https://doi.org/10.1016/j.memsci.2019.03.034.
[21] R.A. Milescu, C.R. McElroy, T.J. Farmer, P.M. Williams, M.J. Walters, J.H. Clark, Fabrication of PES/PVP water filtration membranes using Cyrene®, a safer bio-based polar aprotic solvent, Adv. Polym. Tech. 2019 (2019) e9692859.
[22] S. Mohsenpour, S. Leaper, J. Shokri, M. Alberto, P. Gorgojo, Effect of graphene oxide in the formation of polymeric asymmetric membranes via phase inversion, J. Membr. Sci. 641 (2022), 119924, https://doi.org/10.1016/j.memsci.2021.119924.
[23] S. Lin, S. He, S. Sarwar, R.A. Milescu, C.R. McElroy, S. Dimartino, L. Shao, C. H. Lau, Spray coating polymer substrates from a green solvent to enhance desalination performances of thin film composites, J. Mater. Chem. a. 11 (2023) 891–900, https://doi.org/10.1039/D2TA07200A.
[24] Y. Wibisono, V. Noviani, A.T. Ramadhani, L.A. Devianto, A.A. Sulianto, Eco-friendly forward osmosis membrane manufacturing using dihydrolevoglucosenone, Results Eng. 16 (2022), 100712, https://doi.org/10.1016/j.rineng.2022.100712.
[25] P. Tomietto, F. Russo, F. Galiano, P. Loulergue, S. Salerno, L. Paugam, J.-L. Audic, L. De Bartolo, A. Figoli, Sustainable fabrication and pervaporation application of bio-based membranes: Combining a polyhydroxyalkanoate (PHA) as biopolymer and CyreneTM as green solvent, J. Membr. Sci. 643 (2022), 120061, https://doi.org/10.1016/j.memsci.2021.120061.
[26] D.M. Alonso, S.G. Wettstein, J.A. Dumesic, Gamma-valerolactone, a sustainable platform molecule derived from lignocellulosic biomass, Green Chem. 15 (2013) 584–595, https://doi.org/10.1039/C3GC37065H.
[27] F. Kerkel, M. Markiewicz, S. Stolte, E. Müller, W. Kunz, The green platform molecule gamma-valerolactone – ecotoxicity, biodegradability, solvent properties, and potential applications, Green Chem. 23 (2021) 2962–2976, https://doi.org/10.1039/D0GC04353B.
[28] X. Dong, H.D. Shannon, I.C. Escobar, Investigation of polarclean and gamma-valerolactone as solvents for polysulfone membrane fabrication, in: green polymer chemistry: new products, Processes, and Applications, American Chemical Society, 2018: pp. 385–403. Doi: 10.1021/bk-2018-1310.ch024.
[29] X. Dong, H.D. Shannon, C. Parker, S. De Jesus, I.C. Escobar, Comparison of two low-hazard organic solvents as individual and cosolvents for the fabrication of polysulfone membranes, AIChE J 66 (2020) e16790.
[30] M.A. Rasool, I.F.J. Vankelecom, Use of γ-valerolactone and glycerol derivatives as bio-based renewable solvents for membrane preparation, Green Chem. 21 (2019) 1054–1064, https://doi.org/10.1039/C8GC03652G.
[31] M.A. Rasool, I.F.J. Vankelecom, γ-Valerolactone as bio-based solvent for nanofiltration membrane preparation, Membranes 11 (2021) 418, https://doi.org/10.3390/membranes11060418.
[32] T.A. Tweddle, O. Kutowy, W.L. Thayer, S. Sourirajan, Polysulfone ultrafiltration membranes, Ind. Eng. Chem. Prod. Res. Dev. 22 (1983) 320–326, https://doi.org/10.1021/i300010a030.
[33] T. Ahmad, C. Guria, A. Mandal, Optimal synthesis and operation of low-cost polyvinyl chloride/bentonite ultrafiltration membranes for the purification of oilfield produced water, J. Membr. Sci. 564 (2018) 859–877, https://doi.org/10.1016/j.memsci.2018.07.093.
[34] T. Ahmad, C. Guria, A. Mandal, Optimal synthesis of high fouling-resistant PVC-based ultrafiltration membranes with tunable surface pore size distribution and ultralow water contact angle for the treatment of oily wastewater, Sep. Purif. Technol. 257 (2021), 117829, https://doi.org/10.1016/j.seppur.2020.117829.
[35] T. Ahmad, C. Guria, A. Mandal, Kinetic modeling and simulation of non-solvent induced phase separation: Immersion precipitation of PVC-based casting solution in a finite salt coagulation bath, Polymer 199 (2020), 122527, https://doi.org/10.1016/j.polymer.2020.122527.

[36] T. Ahmad, C. Guria, A. Mandal, Optimal synthesis, characterization and antifouling performance of Pluronic F127/bentonite-based super-hydrophilic polyvinyl chloride ultrafiltration membrane for enhanced oilfield produced water treatment, J. Ind. Eng. Chem. 90 (2020) 58–75, https://doi.org/10.1016/j.jiec.2020.06.023.
[37] T. Ahmad, C. Guria, A. Mandal, Enhanced performance of salt-induced Pluronic F127 and bentonite blended polyvinyl chloride ultrafiltration membrane for the processing of oilfield produced water, J. Water Process Eng. 34 (2020), 101144, https://doi.org/10.1016/j.jwpe.2020.101144.
[38] D. Zuo, B. Zhu, J. Cao, Y. Xu, Influence of alcohol-based nonsolvents on the formation and morphology of pvdf membranes in phase inversion process, Chinese, J. Polym. Sci. 24 (2006) 281–289, https://doi.org/10.1142/S0256767906001308.
[39] P.-Y. Zhang, H. Yang, Z.-L. Xu, Y.-M. Wei, J.-L. Guo, D.-G. Chen, Characterization and preparation of poly(vinylidene fluoride) (PVDF) microporous membranes with interconnected bicontinuous structures via non-solvent induced phase separation (NIPS), J Polym Res. 20 (2013) 66, https://doi.org/10.1007/s10965-012-0066-4.
[40] N. Ali, N.A. Rahim, A. Ali, W. Sani, W. Nik, L.S. Shiung, Effect of ethanol composition in the coagulation bath on membrane performance, J. Appl. Sci. 7 (2007) 2131–2136, https://doi.org/10.3923/jas.2007.2131.2136.
[41] H. Pei, F. Yan, X. Ma, X. Li, C. Liu, J. Li, Z. Cui, B. He, In situ one-pot formation of crown ether functionalized polysulfone membranes for highly efficient lithium isotope adsorptive separation, Eur. Polym. J. 109 (2018) 288–296, https://doi.org/10.1016/j.eurpolymj.2018.10.001.
[42] Y. Tang, J. Sun, S. Li, Z. Ran, Y. Xiang, Effect of ethanol in the coagulation bath on the structure and performance of PVDF-g-PEGMA/PVDF membrane, J. Appl. Polym. Sci. 136 (2019) 47380, https://doi.org/10.1002/app.47380.
[43] S.P. Deshmukh, K. Li, Effect of ethanol composition in water coagulation bath on morphology of PVDF hollow fibre membranes, J. Membr. Sci. 150 (1998) 75–85, https://doi.org/10.1016/S0376-7388(98)00196-3.
[44] C. Zhou, Z. Hou, X. Lu, Z. Liu, X. Bian, L. Shi, L. Li, Effect of polyethersulfone molecular weight on structure and performance of ultrafiltration membranes, Ind. Eng. Chem. Res. 49 (2010) 9988–9997, https://doi.org/10.1021/ie100199h.
[45] S.R. Wickramasinghe, S.E. Bower, Z. Chen, A. Mukherjee, S.M. Husson, Relating the pore size distribution of ultrafiltration membranes to dextran rejection, J. Membr. Sci. 340 (2009) 1–8, https://doi.org/10.1016/j.memsci.2009.04.056.
[46] M. De bruyn, V.L. Budarin, A. Misefari, S. Shimizu, H. Fish, M. Cockett, A.J. Hunt, H. Hofstetter, B.M. Weckhuysen, J.H. Clark, D.J. Macquarrie, Geminal diol of dihydrolevoglucosenone as a switchable hydrotrope: a continuum of green nanostructured solvents, ACS Sustain. Chem. Eng. 7 (2019) 7878–7883. Doi: 10.1021/acssuschemeng.9b00470.
[47] A. Kumar, A. Sharma, B.G. de la Torre, F. Albericio, Scope and Limitations of γ-Valerolactone (GVL) as a green solvent to be used with base for Fmoc removal in solid phase peptide synthesis, Molecules 24 (2019) 4004, https://doi.org/10.3390/molecules24214004.
[48] A. Zhang, H. Bai, L. Li, Breath figure: a nature-inspired preparation method for ordered porous films, Chem. Rev. 115 (2015) 9801–9868, https://doi.org/10.1021/acs.chemrev.5b00069.
[49] S. Krainer, U. Hirn, Contact angle measurement on porous substrates: Effect of liquid absorption and drop size, Colloids Surf. A Physicochem. Eng. Asp. 619 (2021), 126503, https://doi.org/10.1016/j.colsurfa.2021.126503.
[50] G. Arthanareeswaran, S. Velu, L. Muruganandam, Performance enhancement of polysulfone ultrafiltration membrane by blending with polyurethane hydrophilic polymer 31 (2011) 125–131, https://doi.org/10.1515/polyeng.2011.029.
[51] X. Dong, A. Al-Jumaily, I.C. Escobar, Investigation of the use of a bio-derived solvent for non-solvent-induced phase separation (NIPS) fabrication of polysulfone membranes, Membranes 8 (2018) 23, https://doi.org/10.3390/membranes8020023.
[52] S. Habibi, A. Nematollahzadeh, Enhanced water flux through ultrafiltration polysulfone membrane via addition-removal of silica nano-particles: Synthesis and characterization, J. Appl. Polym. Sci. 133 (2016), https://doi.org/10.1002/app.43556.
[53] S. Zhao, Z. Wang, J. Wang, S. Yang, S. Wang, PSf/PANI nanocomposite membrane prepared by in situ blending of PSf and PANI/NMP, J. Membr. Sci. 376 (2011) 83–95, https://doi.org/10.1016/j.memsci.2011.04.008.
[54] C.M. Hansen, Hansen Solubility Parameters: A User's Handbook, Second Edition, 2nd ed., CRC Press, Boca Raton, 2007. Doi: 10.1201/9781420006834.
[55] S.A. Aktij, A. Rahimpour, A. Figoli, Low content nano-polyrhodanine modified polysulfone membranes with superior properties and their performance for wastewater treatment, Environ. Sci.: Nano. 4 (2017) 2043–2054, https://doi.org/10.1039/C7EN00584A.
[56] L. Korson, W. Drost-Hansen, F.J. Millero, Viscosity of water at various temperatures, J. Phys. Chem. 73 (1969) 34–39, https://doi.org/10.1021/j100721a006.
[57] X. Meng, Y. Pu, M. Li, A.J. Ragauskas, A biomass pretreatment using cellulose-derived solvent Cyrene, Green Chem. 22 (2020) 2862–2872, https://doi.org/10.1039/D0GC00661K.
[58] S. Shao, F. Zeng, L. Long, X. Zhu, L.E. Peng, F. Wang, Z. Yang, C.Y. Tang, Nanofiltration membranes with crumpled polyamide films: a critical review on mechanisms, performances, and environmental applications, Environ. Sci. Technol. 56 (2022) 12811–12827, https://doi.org/10.1021/acs.est.2c04736.
[59] A. Ilyas, Y. Hartanto, L.C. Lee, I.F.J. Vankelecom, Micro-patterned cellulose triacetate membranes for forward osmosis: Synthesis, performance and anti-fouling behavior, Desalination 542 (2022), 116076, https://doi.org/10.1016/j.desal.2022.116076.
[60] A. Ilyas, L. Timmermans, M. Vanierschot, I. Smets, I.F.J. Vankelecom, Micro-patterned PVDF membranes and magnetically induced membrane vibration system for efficient membrane bioreactor operation, J. Membr. Sci. 662 (2022), 120978, https://doi.org/10.1016/j.memsci.2022.120978.
[61] M.A. Fox, Flammable Liquids and Class 3, in: M.A. Fox (Ed.), Glossary for the Worldwide Transportation of Dangerous Goods and Hazardous Materials, Springer, Berlin, Heidelberg, 1999, pp. 96–98, https://doi.org/10.1007/978-3-662-11890-0_33.
[62] D. Prat, J. Hayler, A. Wells, A survey of solvent selection guides, Green Chem. 16 (2014) 4546–4551, https://doi.org/10.1039/C4GC01149J.